

Impacts of Nuclear Symmetry Energy on Sound Speeds and Hadron-Quark Phase Transitions via Spinodal Decompositions in Dense Neutron-Rich Matter

Nai-Bo Zhang^{1*} and Bao-An Li^{2†}

¹*School of Physics, Southeast University, Nanjing 211189, China and*

²*Department of Physics and Astronomy, Texas A&M University-Commerce, Commerce, TX 75429-3011, USA*

(Dated: August 2, 2022)

Using a meta model for nuclear Equation of State (EOS) with its parameters constrained by astrophysical observations and terrestrial nuclear experiments, we examine effects of nuclear EOS especially its symmetry energy $E_{\text{sym}}(\rho)$ term on the speed of sound squared $C_s^2(\rho)$ and the hadron-quark transition density ρ_t where $C_s^2(\rho_t)$ vanishes via the spinodal decomposition mechanism in both dense neutron-rich nucleonic matter relevant for relativistic heavy-ion collisions and the $n+p+e+\mu$ matter in neutron stars at β -equilibrium. Unlike in nucleonic matter with fixed values of the isospin asymmetry δ , in neutron stars with a density dependent isospin profile $\delta(\rho)$ determined consistently by the β equilibrium and charge neutrality conditions, the $C_s^2(\rho)$ almost always show a peak and then vanishes at ρ_t strongly depending on the high-density behavior of $E_{\text{sym}}(\rho)$ if the skewness parameter J_0 characterizing the stiffness of high-density symmetric nuclear matter (SNM) EOS is not too far above its currently known most probable value of about -190 MeV inferred from recent Bayesian analyses of neutron star observables. Moreover, in the case of having a super-soft $E_{\text{sym}}(\rho)$ that is decreasing with increasing density above about twice the saturation density of nuclear matter, the ρ_t is significantly lower than the density where the $E_{\text{sym}}(\rho)$ vanishes (indicating the onset of pure neutron matter formation) in neutron star cores.

I. INTRODUCTION

The energy per nucleon $E(\rho, \delta)$ in cold neutron-rich nucleonic matter of density ρ and isospin asymmetry $\delta = (\rho_n - \rho_p)/\rho$ where ρ_n and ρ_p are the densities of neutrons and protons, respectively, can be written as [1]

$$E(\rho, \delta) = E_0(\rho) + E_{\text{sym}}(\rho) \cdot \delta^2 + \mathcal{O}(\delta^4) \quad (1)$$

where $E_0(\rho)$ is the energy per nucleon in symmetric nuclear matter (SNM) while the symmetry energy $E_{\text{sym}}(\rho)$ encodes the energy cost to make the matter more neutron-rich [2]. Both the $E_0(\rho)$ and $E_{\text{sym}}(\rho)$ are important for the stiffness and stability of neutron-rich nuclear matter. For example, within the minimal model of neutron stars consisting of neutrons (n), protons (p), and electrons (e) the incompressibility of n+p+e matter at β equilibrium is approximately [3–5] $K_\mu(\rho) = \rho^2 \frac{d^2 E_0}{d\rho^2} + 2\rho \frac{dE_0}{d\rho} + \delta^2 [\rho^2 \frac{d^2 E_{\text{sym}}}{d\rho^2} + 2\rho \frac{dE_{\text{sym}}}{d\rho} - 2E_{\text{sym}}^{-1}(\rho) (\rho \frac{dE_{\text{sym}}}{d\rho})^2]$. When $K_\mu(\rho)$ is negative the corresponding speed of sound $C_s(\rho)$ become imaginary, indicating the onset of the so-called spinodal decomposition. When this happens, the density fluctuations in the dynamically unstable region grow exponentially. At zero temperature, the K_μ can become negative at both sub-saturation and supra-saturation densities depending on the characteristics of both $E_0(\rho)$ and $E_{\text{sym}}(\rho)$. At low densities, the onset of spinodal decomposition in either the n+p+e matter or purely nucleonic matter is often used to identify the crust-core transition in neutron stars [3–5] or a liquid-gas

phase transition [6–11] related to the nuclear multifragmentation phenomenon in intermediate energy heavy-ion reactions [12–18]. In hot dense hadronic matter formed in relativistic heavy-ion reactions, a high-density spinodal decomposition has been associated with a first-order hadron-quark phase transition, see, e.g., Refs. [19–23]. Many potential signatures of such a transition have been proposed. For example, the resulting time delay of expansion and/or the rapid growth of fluctuations after the spinodal decomposition may lead to the disappearance of elliptic flow [20] or a minimum in the excitation function of collective flow [21, 22] or an enhanced production of composite particles [23] in relativistic heavy-ion collisions. In cold neutron star matter, when the high-density SNM EOS $E_0(\rho)$ is not very stiff and the symmetry energy $E_{\text{sym}}(\rho)$ is very soft, the spinodal decomposition was also found to occur in n+p+e matter at supra-saturation densities indicating possibly a hadron-quark phase transition in the cores of neutron stars [4, 26]. Between the crust-core and hadron-quark transition densities in neutron stars, the K_μ (C_s^2) peaks at certain density depending on the EOS of neutron-rich matter [4]. There have been many extensive studies on the possible first-order phase transition in neutron stars, see, e.g., Refs. [24, 25] for two examples.

While the effects of EOS on the crust-core (liquid-gas) transition density and pressure have been extensively studied, see, e.g., reviews in Ref. [27–30], little is known about the hadron-quark transition density. In fact, determining the latter and the associated phase structures of dense matter has been a long standing goal of both nuclear physics and astrophysics. It is well known that QCD is still facing fundamental difficulties at finite baryon densities to predict accurately the hadron-quark transition density. Often in models considering a first-order hadron-

*naibozhang@seu.edu.cn

†Bao-An.Li@Tamuc.edu

quark phase transition in heavy-ion reactions and/or neutron stars, the transition density ρ_t is normally used as a free model parameter, see, e.g., Refs. [22, 31], that may be inferred from observational data. Sometimes parameterized $C_s(\rho)$ functions are used as inputs in constructing the EOSs to be tested against experimental data. Alternatively, the ρ_t may be obtained by examining the high-density behavior of C_s^2 and its possible vanishing point in the hadronic phase.

In this work, we study the $C_s^2(\rho)$ and the ρ_t via the spinodal decomposition mechanism in both dense neutron-rich nucleonic matter relevant for relativistic heavy-ion collisions and the $n + p + e + \mu$ matter in neutron stars at β -equilibrium using a meta model for nuclear EOS with its parameters constrained by astrophysical observations and terrestrial nuclear experiments. We focus on effects of nuclear EOS especially its symmetry energy $E_{\text{sym}}(\rho)$ term on the $C_s^2(\rho)$ and ρ_t . Because of the long time needed for β -equilibrium, it is the partial derivative of pressure $(\partial P(\rho, \delta)/\partial \rho)_\delta$ at constant δ determines the C_s^2 in relativistic heavy-ion reactions while the $dP(\rho, \delta(\rho))/d\rho$ determines that in neutron stars with their density dependent isospin profile $\delta(\rho)$ determined consistently by the β -equilibrium and charge neutrality conditions. We found that the $C_s^2(\rho)$ in neutron stars almost always show a peak and then vanishes at a ρ_t strongly depending on the high-density behavior of $E_{\text{sym}}(\rho)$ if the skewness parameter J_0 characterizing the stiffness of high-density SNM EOS is not too far above its currently known most probable value of about -190 MeV.

The rest of this paper is organized as follows. In the next section, we summarize the major ingredients and available constraints of a meta EOS model for nucleonic matter and neutron star matter. We also recall definitions of a few relevant physical quantities. We present and discuss our results in section III. We then conclude in section IV.

II. SUMMARY OF A META MODEL EOS FOR NEUTRON-RICH MATTER

In a meta model for neutron-rich matter [32], the SNM EOS $E_0(\rho)$ and symmetry energy $E_{\text{sym}}(\rho)$ in Eq. (1) are parameterized respectively according to

$$E_0(\rho) = E_0(\rho_0) + \frac{K_0}{2} \left(\frac{\rho - \rho_0}{3\rho_0} \right)^2 + \frac{J_0}{6} \left(\frac{\rho - \rho_0}{3\rho_0} \right)^3, \quad (2)$$

where $E_0(\rho_0) = -15.9$ MeV and

$$E_{\text{sym}}(\rho) = E_{\text{sym}}(\rho_0) + L \left(\frac{\rho - \rho_0}{3\rho_0} \right) + \frac{K_{\text{sym}}}{2} \left(\frac{\rho - \rho_0}{3\rho_0} \right)^2 + \frac{J_{\text{sym}}}{6} \left(\frac{\rho - \rho_0}{3\rho_0} \right)^3. \quad (3)$$

Such models have been widely used in Bayesian inferences of nuclear EOS from neutron star observ-

ables or forward modelings of the structures of neutron stars and nuclei as well as their mergers and collisions. The parameters involved have the asymptotic boundary conditions that they become Taylor expansion coefficients when the above parameterizations are used near the saturation density ρ_0 of SNM and $\delta = 0$. Thus, the fiducial values of the incompressibility $K_0 = 9\rho_0^2[\partial^2 E_0(\rho)/\partial \rho^2]|_{\rho=\rho_0}$ and skewness $J_0 = 27\rho_0^3[\partial^3 E_0(\rho)/\partial \rho^3]|_{\rho=\rho_0}$ of SNM EOS $E_0(\rho)$ at ρ_0 , the magnitude $E_{\text{sym}}(\rho_0)$, slope $L = 3\rho_0[\partial E_{\text{sym}}(\rho)/\partial \rho]|_{\rho=\rho_0}$, curvature $K_{\text{sym}} = 9\rho_0^2[\partial^2 E_{\text{sym}}(\rho)/\partial \rho^2]|_{\rho=\rho_0}$ and skewness $J_{\text{sym}} = 27\rho_0^3[\partial^3 E_{\text{sym}}(\rho)/\partial \rho^3]|_{\rho=\rho_0}$ of nuclear symmetry energy $E_{\text{sym}}(\rho)$ at ρ_0 , respectively, from astrophysical observations and terrestrial nuclear experiments provide a guide and some constraints on the parameters of the meta model EOS.

In this work, we fix the low-density EOS parameters at their currently known most probably values, e.g., $K_0 = 240$ MeV [33] and $E_{\text{sym}}(\rho_0) = 31.7$ MeV [34] but vary the high-density parameters within their current uncertain ranges if known. For example, the L parameter is relatively well determined to be around $L = 57.7 \pm 19$ MeV based on surveys of over 80 analyses of various data of nuclear experiments and astrophysical observations available up to 2021 [34–36]. While several analyses have found strong supports for K_{sym} to be around -100 ± 100 MeV [36–39], a larger range is still often used in the literature. As to the J_{sym} parameter, only some theoretical predictions put it in the range between about -200 to $+800$ MeV [40–43]. To our best knowledge, none of the analyses of neither astrophysical nor nuclear physics data has provided a reliable constraint on J_{sym} . Consequently, the high-density behavior of $E_{\text{sym}}(\rho)$ above about $2\rho_0$ is largely open [36, 44].

To see how diverse the meta model $E_{\text{sym}}(\rho)$ can be, a few examples are shown in Fig. 1 by varying the K_{sym} and J_{sym} parameters in their uncertainty ranges discussed above. It is seen that the generated $E_{\text{sym}}(\rho)$

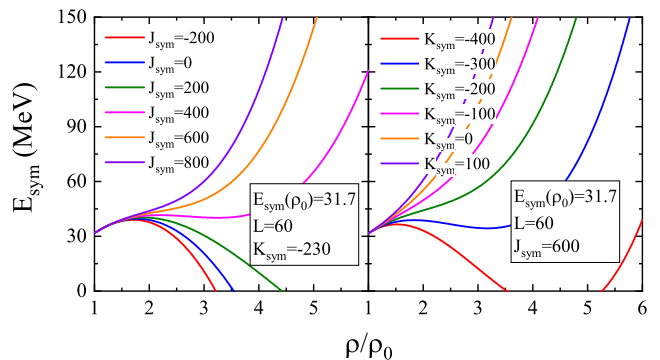


FIG. 1: The density dependences of nuclear symmetry energy with different K_{sym} and J_{sym} values as indicated.

ranges from being super-soft (first increases up to about $2\rho_0$ then start decreasing with increasing density and can even become negative at high densities) to super-

stiff (increases with increasing density much faster than linear). Interestingly, one can even simulate a “cusp” in $E_{\text{sym}}(\rho)$ due to a topology change as predicted by a pseudo-conformal symmetry theory [45]. To our best knowledge, currently neither experimental findings nor fundamental physics principles can rule out any of the high-density behaviors of $E_{\text{sym}}(\rho)$ illustrated in Fig. 1. It has been recognized that the poorly unknown isospin-dependent tensor force and the corresponding short-range nucleon-nucleon correlation as well as the spin-isospin dependence of three-body force in neutron-rich matter are among the most important origins of the wide open behavior of high-density symmetry energy [46]. Impacts of the diverse high-density behaviors of $E_{\text{sym}}(\rho)$ on properties of neutron stars and heavy-ion collisions have also been studied in several works, see, e.g., Refs. [36, 45–55].

On the other hand, there are several available constraints on the J_0 parameter which characterizes the stiffness of SNM EOS at densities above about $(2-3)\rho_0$. For example, recent Bayesian analyses of neutron star radii from LIGO and NICER observations have inferred the most probable value of J_0 to be about $J_0 = -190_{-40}^{+40}$ at 68% confidence level [56, 57]. While its most probable value extracted from a Bayesian analysis of nuclear collective flow in relativistic heavy-ion collisions is $J_0 = -180_{-110}^{+100}$ MeV at 68% confidence level [58]. Moreover, it was found that to support a neutron star of mass $2.17 M_\odot$ a minimum value of about $J_0 = -180$ MeV is needed [59]. While the causality requirement can provide an upper limit on J_0 , the range of about $-90 < J_0 < 200$ MeV obtained in this way depends strongly on the correlation between the high-density SNM EOS and symmetry energy [59]. We will thus explore effects of J_0 in a large range around its most probable value of about -190 MeV.

The energy density in neutron stars consisting of neutrons, protons, electrons, and muons at β -equilibrium is given by

$$\epsilon(\rho, \delta) = \rho[E(\rho, \delta) + M_N] + \epsilon_l(\rho, \delta), \quad (4)$$

where M_N represents the average nucleon mass and $\epsilon_l(\rho, \delta)$ denotes the lepton energy density. The pressure is then

$$P(\rho, \delta) = \rho^2 \frac{d\epsilon(\rho, \delta)/\rho}{d\rho}. \quad (5)$$

The pressure in neutron stars at β -equilibrium becomes barotropic once the density-profile of the isospin asymmetry $\delta(\rho)$ is obtained self-consistently from the β -equilibrium condition

$$\mu_n - \mu_p = \mu_e = \mu_\mu \approx 4\delta E_{\text{sym}}(\rho) \quad (6)$$

and the charge neutrality condition $\rho_p = \rho_e + \rho_\mu$. The chemical potential μ_i for a particle i is obtained from $\mu_i = \partial\epsilon(\rho, \delta)/\partial\rho_i$. We notice that in nucleonic matter at fixed isospin asymmetries relevant for heavy-ion reactions, the nucleonic part of the above equations gives the corresponding pressure $P(\rho, \delta)$.

For easy of our following discussions, it is useful to recall that the pressure in the n+p+e model of neutron stars is given by [60]

$$P(\rho, \delta) = \rho^2 \left[\frac{dE_{\text{SNM}}(\rho)}{d\rho} + \frac{dE_{\text{sym}}(\rho)}{d\rho} \delta^2 \right] + \frac{1}{2} \delta(1-\delta)\rho E_{\text{sym}}(\rho) \quad (7)$$

and the isospin profile $\delta(\rho)$ (or the corresponding proton fraction $x_p(\rho) = (1-\delta)/2$) at β -equilibrium is determined completely by the $E_{\text{sym}}(\rho)$ via

$$x_p(\rho) = 0.048 [E_{\text{sym}}(\rho)/E_{\text{sym}}(\rho_0)]^3 (\rho/\rho_0)(1 - 2x_p(\rho))^3. \quad (8)$$

Based on this equation and as we shall illustrate numerically, as the $E_{\text{sym}}(\rho)$ goes to zero at high densities in the case of a super-soft symmetry energy, the δ approaches 1 and if the $E_{\text{sym}}(\rho)$ is super-stiff the resulting δ will vanish at very high densities.

As the speed of sound $C_s(\rho)$ is a measure of the stiffness of nuclear EOS, its high-density behavior is largely controlled by the skewness J_0 of SNM EOS as well as the curvature K_{sym} and skewness J_{sym} of nuclear symmetry energy. Through the charge neutrality and β -equilibrium conditions, the K_{sym} and J_{sym} also determine the high-density behavior of the isospin profile $\delta(\rho)$ of neutron stars. As we shall discuss, the $\delta(\rho)$ plays a significant role in determining the density dependence of the sound speed $C_s(\rho)$ and its possible vanishing point ρ_t . In the following, we denote the speed of sound squared in nucleonic matter of fixed isospin asymmetry δ with C_{NM}^2 (the so-called adiabatic speed), and that in neutron stars at β -equilibrium with C_s^2 (the so-called equilibrium sound speed). More specifically, they are respectively defined by

$$C_{NM}^2 \equiv \left(\frac{\partial P}{\partial \epsilon} \right)_\delta \quad \text{and} \quad C_s^2 \equiv \frac{dP}{d\epsilon}. \quad (9)$$

It has been shown earlier that in terms of the pressure P and incompressibility $K \equiv 9 \left(\frac{\partial P}{\partial \rho} \right)_\delta$, the adiabatic sound speed in unit of c^2 in nuclear matter can be rewritten as [39, 61, 62]

$$C_{NM}^2 = \frac{K}{9(M_N + E(\rho, \delta) + P/\rho)}. \quad (10)$$

Since the density profile $\delta(\rho)$ has to be calculated numerically above the μ production threshold, no analytical expression for the C_s^2 is available. We notice that one can also calculate the speed of sound in neutron stars at a fixed isospin asymmetry, namely the so-called adiabatic speed of sound in studying the g-mode of neutron star oscillations [63] and its dependence on the $E_{\text{sym}}(\rho)$ [29, 62, 64, 65]. While a fluid element in a neutron star in a g-mode oscillation is always in mechanical equilibrium with the surroundings, its composition stays a constant during the adiabatic process because the weak interaction timescale leading to β -equilibrium is much

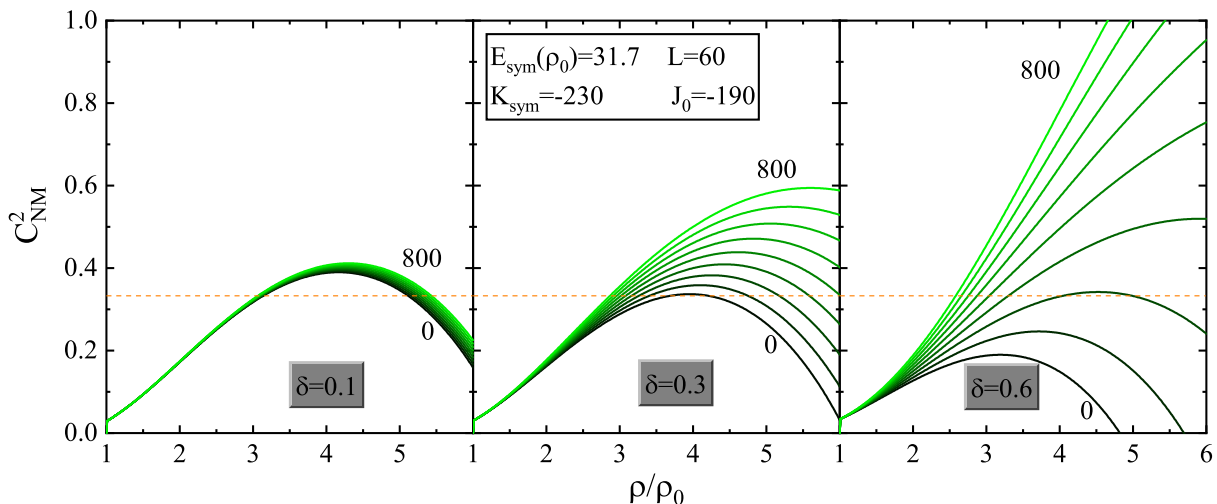


FIG. 2: The speed of sound C_{NM}^2 in unit of c^2 in nucleonic matter with fixed isospin asymmetries as a function of density using the symmetry energy $E_{\text{sym}}(\rho)$ functions with J_{sym} varying between 0 and 800 MeV as shown in the left panel of Fig. 1.

longer than the dynamical timescale. The difference between the adiabatic and equilibrium sound speeds determines the g-mode frequency. In fact, the high-density behavior of $E_{\text{sym}}(\rho)$ was found to have a significant effect on the g-mode frequency, see, e.g., Ref. [62] and the review in Section 7.1 of Ref. [29].

We notice that there are many interesting studies on the sound speed in different phases of dense matter or neutron stars assumed to have multiple components under various conditions, see, e.g., Refs. [39, 45, 64–77] and references therein. As outlined above, our main goal here is rather conservative. We focus on studying the density dependence of the sound speed in purely nucleonic matter or the $n + p + e + \mu$ matter and its possible vanishing point ρ_t as the transition point to the quark phase. The ρ_t obtained in this way may be used as an input in constructing more complicated EOSs to study some of the interesting and unresolved issues about the phase diagram of dense neutron-rich matter.

III. RESULTS AND DISCUSSIONS

In the following, we present our results on the speeds of sound in nucleonic matter and neutron star matter separately. We examine effects of the EOS parameters on the density dependence of the speeds of sound and their possible vanishing points.

A. Speed of sound in neutron-rich nucleonic matter with fixed isospin asymmetries

Shown in Fig. 2 is the speed of sound C_{NM}^2 in nucleonic matter with fixed isospin asymmetries of $\delta = 0.1, 0.3$ and 0.6 , respectively, as a function of density using the symmetry energy $E_{\text{sym}}(\rho)$ functions with J_{sym} varying

between 0 and 800 MeV as shown in the left panel of Fig. 1. All other EOS parameters are fixed at their currently known most probable values as we discussed earlier. As one expects, as the matter becomes more neutron-rich, effects of J_{sym} become larger. Interestingly, with relatively small δ and/or J_{sym} values the C_{NM}^2 shows a peak. From inspecting the expression of Eq. (10) for C_{NM}^2 in the limiting case of SNM, one can see that while the denominator keeps increasing with density, the incompressibility K in the numerator peaks at certain density since the K_0 is positive but J_0 is negative. Thus, the C_{NM}^2 in SNM normally has a peak. With the parameters L and K_{sym} fixed, the isospin asymmetric energy, pressure, and its derivative all increase with positive and increasing J_{sym} . Their net effect is adding a positive and continuously increasing contribution to C_{NM}^2 , making its peak disappears gradually when the $E_{\text{sym}}(\rho)$ becomes very stiff for large J_{sym} values. Of course, if one uses negative J_{sym} values leading to super-soft $E_{\text{sym}}(\rho)$ functions, the C_{NM}^2 not only has a peak but also vanishes at a lower density ρ_t as we shall discuss next.

As shown in Fig. 1, with small or negative J_{sym} values, the $E_{\text{sym}}(\rho)$ is super-soft and vanishes at some point or becomes negative at higher densities. It is thus interesting to compare the hadron-quark transition density ρ_t where $C_{NM}^2(\rho_t)=0$ and the critical density where $E_{\text{sym}}(\rho)=0$. It is known that a vanishing $E_{\text{sym}}(\rho)$ in nucleonic matter indicates the onset of the so-called isospin separation instability, namely it is energetically more favorable to split SNM into pure neutron matter and proton matter when the $E_{\text{sym}}(\rho)$ becomes negative [47, 50]. Its possible ramifications in heavy-ion reactions and neutron stars have been studied in several works, see., e.g., Refs. [36, 45–55].

Shown in Fig. 3 is a comparison of the two transition densities where either $C_{NM}^2(\rho_t)=0$ or $E_{\text{sym}}(\rho)=0$ as a function of K_{sym} with several small J_{sym} values all

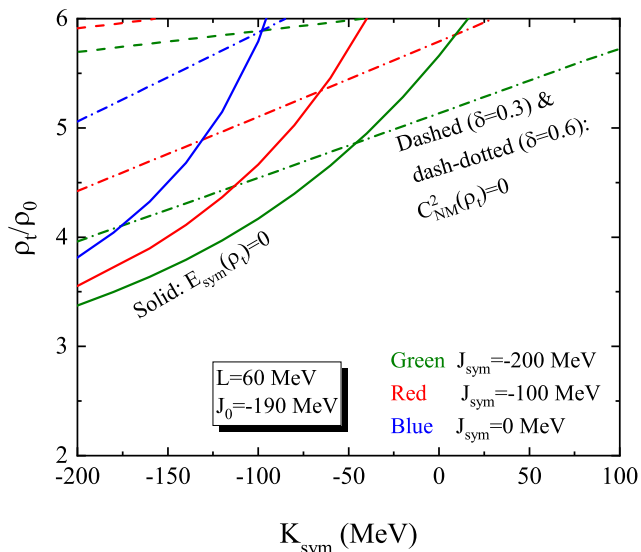


FIG. 3: A comparison of the hadron-quark transition density ρ_t where $C_{NM}^2(\rho_t)=0$ and the critical density where $E_{\text{sym}}(\rho)=0$ indicating the onset of isospin separation instability with EOS parameters leading to super-soft symmetry energies.

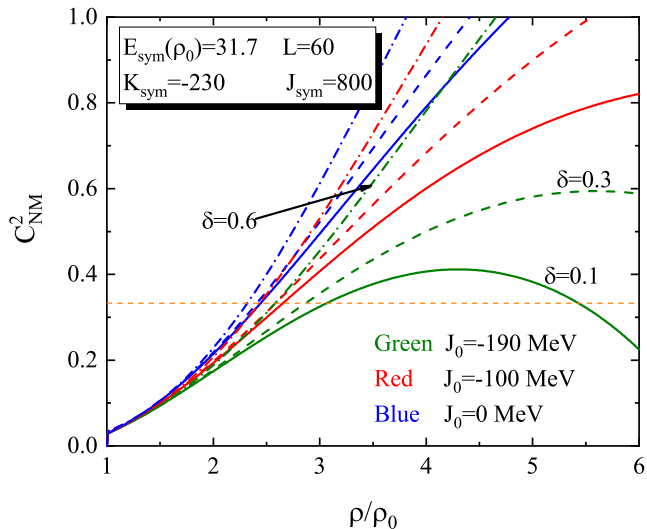


FIG. 4: Effects of J_0 characterizing the stiffness of SNM EOS on the speed of sound in nucleonic matter with the $E_{\text{sym}}(\rho)$ parameters fixed at the values specified leading to a stiff $E_{\text{sym}}(\rho)$ function. The solid, dashed and dot-dashed lines are for $\delta = 0.1, 0.3$ and 0.6 , respectively.

leading to super-soft $E_{\text{sym}}(\rho)$ functions. As illustrated in Fig. 1, it is the combination of K_{sym} and J_{sym} that is determining the high-density behavior of $E_{\text{sym}}(\rho)$ above about $2\rho_0$. It is seen that when both the K_{sym} and J_{sym} are small leading to very soft $E_{\text{sym}}(\rho)$ functions that vanish quickly, the critical density for $E_{\text{sym}}(\rho)=0$ is smaller than that for $C_{NM}^2(\rho_t)=0$ for a given value of J_{sym} and δ . Unless the matter is very neutron-rich (with $\delta \geq 0.6$) and the K_{sym} is positive, the hadron-quark transition will

not happen before the isospin separation occurs as one moves from low to high densities. Since most of the existing analyses support $K_{\text{sym}} \approx -100 \pm 100$ MeV at 68% confidence level and if indeed the J_{sym} is small, a super-soft $E_{\text{sym}}(\rho)$ is realized, and then the isospin separation occurs first. However, as we discussed earlier, there is currently no experimental constraint on the J_{sym} , leaving all possibilities open. Thus, our findings here add more importance for constraining the high-density behavior of nuclear symmetry energy especially its skewness parameter J_{sym} .

In the results presented above, we have used the currently known most probable value of -190 MeV for the skewness parameter J_0 of SNM EOS. As we discussed earlier, the J_0 still has a large uncertainty range. To reveal its quantitative effects on the speed of sound, we vary J_0 between 0 and -190 MeV using a relatively stiff $E_{\text{sym}}(\rho)$ function created with $K_{\text{sym}} = -230$ MeV and $J_{\text{sym}} = 800$ MeV. The results are shown in Fig. 4. It is seen that the peak in the speed of sound gradually disappears if the J_0 is far from its most probable value of -190 MeV such that the SNM EOS becomes very stiff at high densities. This effect is stronger for more neutron-rich matter as a very large J_{sym} of 800 MeV is used. These features are easily understood from the terms involved in the expression for C_{NM}^2 in Eq. (10).

In short, in nucleonic matter with fixed isospin asymmetries, if the J_0 is close to its most probable value of -190 MeV and the $E_{\text{sym}}(\rho)$ is not too stiff, the $C_{NM}^2(\rho)$ shows a peak and may become zero at high densities. However, if the $E_{\text{sym}}(\rho)$ is super-stiff especially with high isospin asymmetries the $C_{NM}^2(\rho)$ will keep increasing with density until reaching the causality limit. As we shall illustrate and discuss next, the physical consequence of the last case will be changed completely when the β -equilibrium condition is introduced in building the EOS for neutron stars.

B. Speed of sound in charge neutral $npe\mu$ matter in neutron stars at β -equilibrium

Besides the contributions from leptons, the most important difference between the EOSs of nucleonic matter at fixed δ and neutron star matter is the consequence of charge neutrality and β -equilibrium in the latter. It is well known that in neutron stars at β -equilibrium, the isospin profile $\delta(\rho)$ is uniquely determined by the Eq.(6). As mentioned earlier, the resulting $\delta(\rho)$ approaches one (zero) when the $E_{\text{sym}}(\rho)$ becomes zero (very high or stiff). This result is also easy to understand qualitatively from the energy conservation point of view. As shown in Eq. (1), the $E(\rho, \delta) \propto E_{\text{sym}}(\rho) \cdot \delta^2$. To conserve the total energy, if the $E_{\text{sym}}(\rho)$ is high (low) at certain density ρ the $\delta(\rho)$ there will be low (high). In both cases, the same isospin asymmetry δ of the whole system is just being distributed to different density regions according to the well-known isospin fractionation mech-

anism in asymmetric nuclear matter [11, 78–81]. Considering two connected regions with local densities ρ_1 and ρ_2 , respectively, the chemical equilibrium condition requires $E_{\text{sym}}(\rho_1)\delta(\rho_1) = E_{\text{sym}}(\rho_2)\delta(\rho_2)$. Thus, for a given $E_{\text{sym}}(\rho)$ function, the local isospin asymmetries will adjust themselves according to the relative symmetry energy in those regions.

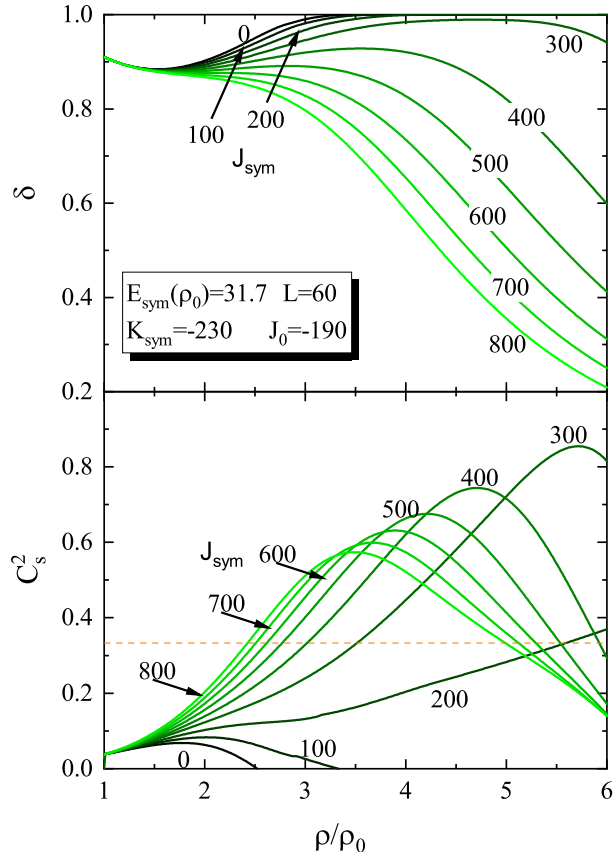


FIG. 5: The density profile of isospin asymmetry $\delta(\rho)$ (upper panel) and the corresponding sound speed squared $C_s^2(\rho)$ in unit of c^2 in neutron stars at β -equilibrium with J_{sym} varying between 0 and 800 MeV but other parameters fixed at their currently known most probable values indicated.

Shown in Fig. 5 are the density profile of isospin asymmetry $\delta(\rho)$ (upper panel) and the corresponding squared speed of sound in neutron stars at β -equilibrium with J_{sym} varying between 0 and 800 MeV but other parameters fixed at their currently known most probable values. Again, the corresponding $E_{\text{sym}}(\rho)$ is the one shown in the left panel of Fig. 1. Indeed, it is seen that the super-stiff $E_{\text{sym}}(\rho)$ with $J_{\text{sym}}=800$ MeV leads to a vanishing δ (SNM) at high densities. While the super-soft $E_{\text{sym}}(\rho)$ with $J_{\text{sym}}=0$ leads to $\delta = 1$ (pure neutron matter) at high densities. Namely, in both cases the product of $E_{\text{sym}}(\rho)$ and δ at high densities reach zero as required by the β -equilibrium and charge neutrality conditions.

Consequently, regardless of the high-density behavior of $E_{\text{sym}}(\rho)$ (super-soft or super-stiff), the equilibrium speed of sound $C_s^2(\rho)$ in neutron stars at β -equilibrium always show a peak with its position depends on the values of J_{sym} and other EOS parameters as we shall discuss in more detail. Therefore, compared to the results shown in the previous subsection, it is clearly seen that the high-density behaviors of sound speeds in neutron stars at β -equilibrium and nucleonic matter with fixed δ values are very different.

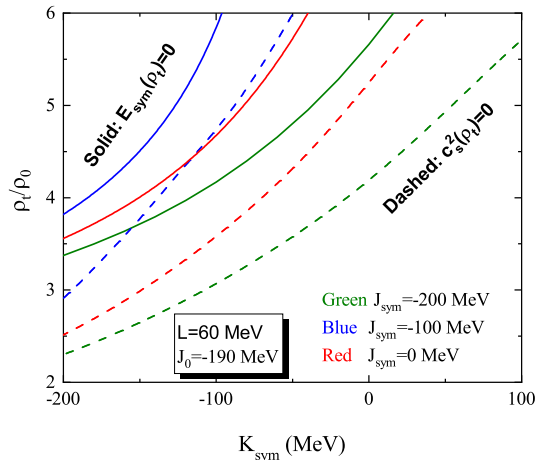


FIG. 6: A comparison of the critical densities where the symmetry energy $E_{\text{sym}}(\rho) = 0$ with that where the sound speed $C_s^2 = 0$ as functions of K_{sym} with $J_{\text{sym}} = 0, -100$ and -200 MeV, respectively, and all other parameters fixed at their currently known most probable values.

Again, it is interesting to compare the critical density where the symmetry energy $E_{\text{sym}}(\rho) = 0$ with that where the sound speed $C_s^2 = 0$ in the case of having super-soft $E_{\text{sym}}(\rho)$ functions. Shown in Fig. 6 are the two critical densities as functions of K_{sym} with $J_{\text{sym}} = 0, -100$ and -200 MeV, respectively, and all other parameters fixed at their currently known most probable values. It is seen that in the whole EOS parameter space considered, the hadron-quark phase transition density ρ_t is always lower than the critical density where $E_{\text{sym}}(\rho) = 0$. Consequences and/or observational evidences of this finding deserve further studies.

C. Hadron-quark transition density via spinodal decomposition in neutron stars at β -equilibrium

We now focus on examining the hadron-quark transition density ρ_t where $C_s^2(\rho_t) = 0$. First, we fix the J_0 at its most probable value of -190 MeV and study the dependence of ρ_t on the slope L , curvature K_{sym} , and skewness J_{sym} parameters of $E_{\text{sym}}(\rho)$ within their current uncertainty ranges in Fig. 7. Overall, a softer $E_{\text{sym}}(\rho)$ leads to a smaller ρ_t . Approaching the lower

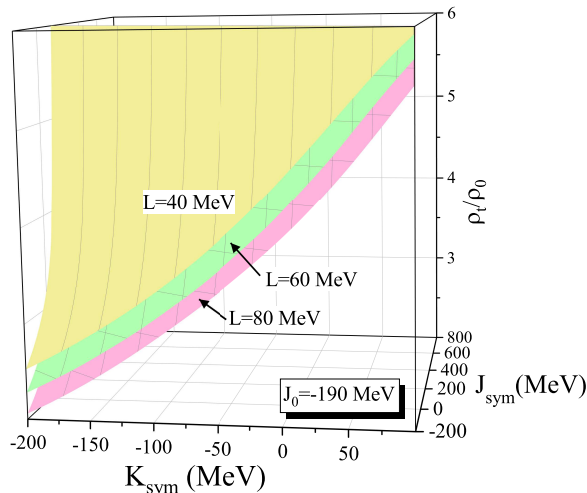


FIG. 7: The hadron-quark transition density in 3D as a function of J_{sym} and K_{sym} with $L = 40, 60,$ and 80 MeV, respectively. All other parameters are fixed at their currently known most probable values.

limits of K_{sym} and J_{sym} where the $E_{\text{sym}}(\rho)$ is super-soft, the ρ_t can be as low as about $2\rho_0$. Such a low hadron-quark phase transition density is actually consistent with its lower boundary inferred from several recent Bayesian analyses of neutron star observables [82–86]. However, at the other limit where both the K_{sym} and J_{sym} take large positive values, the $E_{\text{sym}}(\rho)$ is super-stiff and the resulting ρ_t is about $(5 - 6)\rho_0$. It is also seen that varying the L parameter from 40 to 80 MeV causes an approximately 30% change in ρ_t . The wide range of ρ_t due to the uncertainty of the $E_{\text{sym}}(\rho)$ especially at high densities signifies again the need to better constrain the density dependence of nuclear symmetry energy.

Next, we examine in Fig. 8 effects of J_0 on ρ_t while the $E_{\text{sym}}(\rho)$ parameters are also varied around their most probable values. For exploration purposes only, in one of the calculations we purposely used a very low J_0 of -290 MeV leading to an EOS that is not stiff enough to support a neutron star of mass $2.01 M_{\odot}$. We also extended the lower limit of K_{sym} to -400 MeV that is far below its 1σ lower boundary of $K_{\text{sym}} \approx -100 \pm 100$ MeV from several surveys of its constraints in the literature [36]. It is seen that even with such a low K_{sym} (which controls the behavior of $E_{\text{sym}}(\rho)$ around $(1 - 2)\rho_0$ value, the hadron-quark transition may still happen at densities below about $(1.5 - 3)\rho_0$. However, as the K_{sym} increases in the case of using a very stiff SNM EOS (e.g., with $J_0 = -90$ MeV shown in the left panel far above its most likely value of -190 MeV used in the middle panel) and a large J_{sym} , the hadron-quark transition may not occur as indicated by the ending of the ρ_t curves with $J_{\text{sym}}=200$

MeV in the left panel.

At the other extreme of using a very soft SNM EOS with $J_0 = -290$ MeV shown in the right panel), the transition density is again dominated by the SNM EOS and becomes less dependent on the $E_{\text{sym}}(\rho)$ as indicated by the tendency of saturation at the high K_{sym} limit in the right panel in Fig. 8. These features indicate that there are strong interplays and correlations among the SNM EOS and $E_{\text{sym}}(\rho)$ parameters as one expects.

In short, unlike in nucleonic matter with fixed δ values, the speed of sound in neutron stars at β -equilibrium almost always show a peak as long as the J_0 characterizing the stiffness of high-density SNM EOS is not too far above its currently known most probable value of about -190 MeV. Moreover, the hadron-quark transition density ρ_t from the spinodal decomposition mechanism strongly depends on the high-density behavior of nuclear symmetry energy $E_{\text{sym}}(\rho)$.

IV. SUMMARY

In summary, within a meta EOS model we studied the speed of sound and the possible hadron-quark transition in both nucleonic matter with fixed isospin asymmetries and the $n + p + e + \mu$ matter in neutron stars at β -equilibrium. While in nucleonic matter with fixed isospin asymmetries the speed of sound may continuously increase with density and does not undergo a spinodal decomposition especially for neutron-rich matter if the $E_{\text{sym}}(\rho)$ is very stiff, the sound speed in neutron star matter at β -equilibrium almost always show a peak at certain density depending strongly on the high-density behavior of $E_{\text{sym}}(\rho)$ if the skewness J_0 of SNM EOS is not too far above its currently known most probable value of about -190 MeV. Moreover, the corresponding hadron-quark transition density from the spinodal decomposition mechanism depends sensitively on the high-density behavior of nuclear symmetry energy $E_{\text{sym}}(\rho)$. Furthermore, in the case of using a super-soft $E_{\text{sym}}(\rho)$, the hadron-quark transition occurs at a density lower than the critical density above which the neutron star cores become pure neutron matter.

Acknowledgments

This work is supported in part by the U.S. Department of Energy, Office of Science, under Award Number DE-SC0013702, the CUSTIPEN (China-U.S. Theory Institute for Physics with Exotic Nuclei) under the US Department of Energy Grant No. DE-SC0009971, the National Natural Science Foundation of China under Grant No. 12005118, and the Shandong Provincial Natural Science Foundation under Grants No. ZR2020QA085.

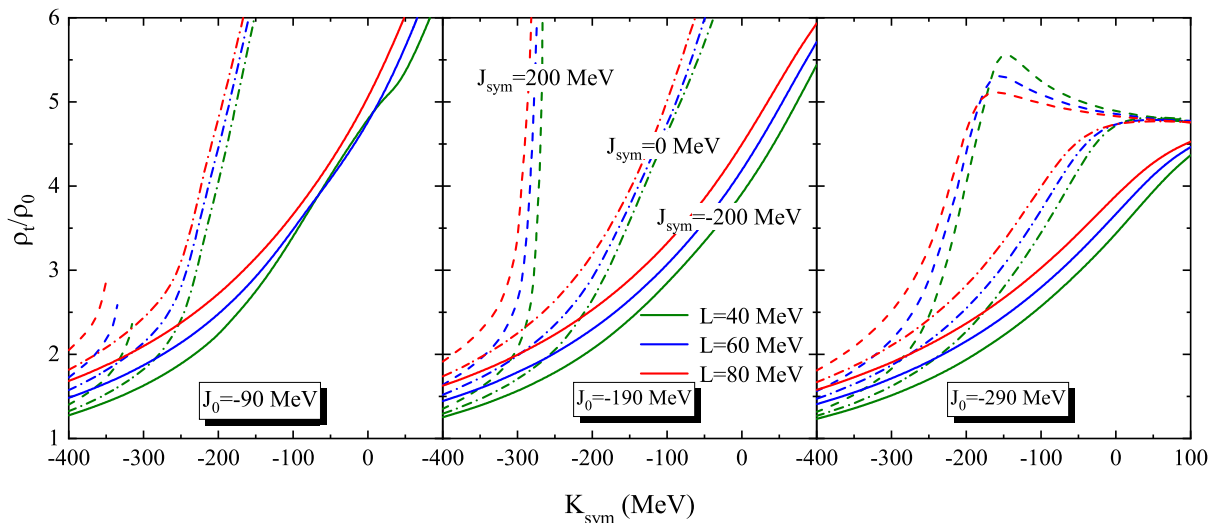


FIG. 8: Effects of the skewness J_0 of SNM EOS on the hadron-quark transition density in neutron stars at β -equilibrium through the spinodal decomposition mechanism.

-
- [1] I. Bombaci, U. Lombardo, Phys. Rev. C **44**, 1892 (1991).
- [2] B. A. Li, À. Ramos, G. Verde, and I. Vidaña (Eds.), *Topical issue on nuclear symmetry energy*, Eur. Phys. J. A **50**, No.2 (2014).
- [3] J. M. Lattimer and M. Prakash, Phys. Rep. **333**, 121 (2000).
- [4] S. Kubis, Phys. Rev. C **76**, 025801 (2007).
- [5] J. Xu, L.W. Chen, B.A. Li, H.R. Ma, Astrophys. J. **697**, 1549 (2009).
- [6] G. F. Bertsch and P. J. Siemens, Phys. Lett. B **126**, 9 (1983).
- [7] P. J. Siemens, Nature **305**, 410 (1983).
- [8] J. A. Lopez and P. J. Siemens, Nucl. Phys. A **431**, 728 (1984).
- [9] L. Goodman, J. I. Kapusta, and A. Z. Mekjian, Phys. Rev. C **30**, 851 (1984).
- [10] B. A. Li, S. Pratt, and P. J. Siemens, Phys. Rev. C **37**, 728 (1988).
- [11] H. Muller and B. D. Serot, Phys. Rev. C **52**, 2072-2091 (1995).
- [12] L. G. Moretto, K. Tso, N. Colonna, and G. J. Wozniak, Phys. Rev. Lett. **69**, 1884 (1992).
- [13] W. Bauer, G. F. Bertsch, and H. Schulz, Phys. Rev. Lett. **69**, 1888 (1992).
- [14] B. A. Li and D. H. E. Gross, Nucl. Phys. A **554**, 257 (1993).
- [15] H. M. Xu, J. B. Natowitz, C. A. Gagliardi, R. E. Tribble, C. Y. Wong and W. G. Lynch, Phys. Rev. C **48**, 933-936 (1993)
- [16] P. Chomaz, M. Colonna, and J. Randrup, Phys. Rep. **389**, 263 (2004).
- [17] M. Colonna, Prog. Part. Nucl. Phys. **113**, 103775 (2020).
- [18] P. Danielewicz, H. Lin, J. R. Stone, and Y. Iwata, Phys. Lett. B **811**, 135957 (2020).
- [19] D. H. Rischke and M. Gyulassy, Nucl. Phys. A **597**, 701 (1996).
- [20] P. Danielewicz, R. A. Lacey, P. B. Gossiaux, C. Pinkenburg, P. Chung, J. M. Alexander and R. L. McGrath, Phys. Rev. Lett. **81**, 2438-2441 (1998)
- [21] D. H. Rischke, Y. Pürsün, J. A. Maruhn, H. Stoecker and W. Greiner, Acta Phys. Hung. A **1**, 309-322 (1995)
- [22] B. A. Li and C. M. Ko, Phys. Rev. C **58**, R1382 (1998).
- [23] J. Steinheimer and J. Randrup, Phys. Rev. Lett. **109**, 212301 (2012).
- [24] N. K. Glendenning, Phys. Rev. D **46**, 1274-1287 (1992).
- [25] H. Tan, T. Dore, V. Dexheimer, J. Noronha-Hostler and N. Yunes, Phys. Rev. D **105**, no.2, 023018 (2022).
- [26] B. A. Li and M. Magno, Phys. Rev. C **102**, 045807 (2020).
- [27] B. A. Li, L. W. Chen, and C. M. Ko, Phys. Rep. **464**, 113 (2008).
- [28] C. Providência, S. S. Avancini, R. Cavagnoli, S. Chiacchiera, C. Ducoin, F. Grill, J. Margueron, D. P. Menezes, A. Rabhi, and I. Vidaña, Euro. Phys. J. A **50**, 44 (2014).
- [29] B. A. Li, P. G. Krastev, D. H. Wen, and N. B. Zhang, Euro. Phys. J. A **55**, 117 (2019).
- [30] M. Ferreira, A. Rabhi, and C. Providência, Eur. Phys. J. A **57**, 263 (2021).
- [31] M. G. Alford, S. Han, and M. Prakash, Phys. Rev. D **88**, 083013 (2013).
- [32] N.B. Zhang, B.A. Li and J. Xu, Astrophysical J. **859**, 90 (2018).
- [33] U. Garg and G. Colò, Prog. Part. Nucl. Phys. **101**, 55(2018).
- [34] B. A. Li and X. Han, Phys. Lett. B **727**, 276 (2013).
- [35] M. Oertel, M. Hempel, T. Klähn, and S. Typel, Rev. Mod. Phys. **89**, 015007 (2017).
- [36] B. A. Li, B. J. Cai, W. J. Xie, and N. B. Zhang, Universe **7**, 182 (2021).
- [37] C. Mondal, B. K. Agrawal, J. N. De, S. K. Samaddar, M. Centelles, and X. Viñas, Phys. Rev. C **96**, 021302 (2017).
- [38] J. Margueron, R. H. Casali, and F. Gulminelli, Phys. Rev. C **97**, 025806 (2018).
- [39] G. Grams, R. Somasundaram, J. Margueron, and E. Khan, arXiv:2207.01884.
- [40] M. Dutra, O. Louren, J. S. S. Martins, A. Delfino, J. R.

- Stone, and P. D. Stevenson, *Phys. Rev. C* **85**, 035201 (2012).
- [41] M. Dutra, O. Lourenço, S. S. Avancini, B. V. Carlson, A. Delfino, D. P. Menezes, C. Providência, S. Typel, and J. R. Stone, *Phys. Rev. C* **90**, 055203 (2014).
- [42] I. Tews, J. M. Lattimer, A. Ohnishi, and E. E. Kolomeitsev, *Astrophys. J.* **848**, **105** (2017).
- [43] N. B. Zhang, B. J. Cai, B. A. Li, W. G. Newton, and J. Xu, *Nucl. Sci. Tech.* **28**, 181 (2017).
- [44] N. B. Zhang and B. A. Li, *Astrophys. J.* **921**, 111 (2021).
- [45] H. K. Lee, Y. L. Ma, W. G. Paeng, and M. Rho, *Mod. Phys. Lett. A* **37**, 2230003 (2022).
- [46] B. J. Cai and B. A. Li, [arXiv:2206.15314 [nucl-th]], *Annals of Physics* in press, <https://doi.org/10.1016/j.aop.2022.169062>
- [47] M. Kutschera and W. Wójcik, *Phys. Rev. C* **47**, 1077 (1993).
- [48] M. Kutschera, *Phys. Lett. B* **340**, 1 (1994).
- [49] A. Szmagliński, W. Wójcik, and M. Kutschera., *Acta Phys. Pol. B* **37**, 277 (2006).
- [50] B. A. Li, *Phys. Rev. Lett.* **88**, 192701 (2002).
- [51] D. H. Wen, B. A. Li, and L. W. Chen, *Phys. Rev. Lett.* **103**, 211102 (2009).
- [52] D. T. Khoa, W. von Oertzen, and A. A. Ogloblin, *Nucl. Phys. A* **602**, 98 (1996).
- [53] D. N. Basu, P. Roy Chowdhury, and C. Samanta, *Nucl. Phys. A* **811**, 140 (2008).
- [54] S. Banik and D. Bandyopadhyay, *J. Phys. G* **26**, 1495 (2000).
- [55] S. Kubis and M. Kutschera, *Nucl. Phys. A*, **720**, 189 (2003).
- [56] W. J. Xie and B. A. Li, *Astrophys. J.* **883**, 174 (2019).
- [57] W. J. Xie and B. A. Li, *Astrophys. J.* **899**, 4 (2020).
- [58] W. J. Xie and B. A. Li, *J. Phys. G* **48**, 025110 (2021).
- [59] N. B. Zhang and B. A. Li, *Astrophys. J.*, **879**, 99 (2019).
- [60] J. M. Lattimer and M. Prakash, *Astrophys. J.* **550**, 426 (2001).
- [61] J. P. Blaizot, *Phys. Rep.* **64**, 171 (1980).
- [62] D. Lai, *Mon. Not. R. Astron. Soc.* **270**, 611 (1994).
- [63] A. Reisenegger and P. Goldreich, *Astrophys. J.* **395**, 240 (1992).
- [64] T. Malik, M. Ferreira, B. K. Agrawal, and C. Providência, *Astrophys. J.* **930**, 17 (2022).
- [65] N. Lozano, V. Tran, and P. Jaikumar, *Galaxies* **10**, 79 (2022)
- [66] L. McLerran and S. Reddy, *Phys. Rev. Lett.* **122**, 122701 (2019).
- [67] H. Tan, V. Dexheimer, J. Noronha-Hostler, and N. Yunes, *Phys. Rev. Lett.* **128**, 161101 (2022).
- [68] C. Drischler, S. Han, and S. Reddy, *Phys. Rev. C* **105**, 035808 (2022).
- [69] R. M. Aguirre, *Phys. Rev. D* **105**, 116023 (2022).
- [70] S. Altiparmak, C. Ecker, and L. Rezzolla, arXiv:2203.14974.
- [71] J. Braun, A. Geißel, and B. Schallmo, arXiv:2206.06328.
- [72] A. Kanakis-Pegios, P. S. Koliogiannis, and C. C. Moustakidis, *Phys. Rev. C* **102**, 055801 (2020).
- [73] T. Kojo, *AAPPS Bull.* **31**, 11 (2021).
- [74] T. F. Motta, P. A. M. Guichon, and A. W. Thomas, *Nucl. Phys. A* **1009**, 122157 (2021).
- [75] M. Marczenko, L. McLerran, K. Redlich, and C. Sasaki, arXiv:2207.13059.
- [76] D. Kumar, H. Mishra, and T. Malik, arXiv:2110.00324.
- [77] M. Z. Han, Y. J. Huang, S. P. Tang, and Y. Z. Fan, arXiv:2207.13613.
- [78] B. A. Li and C. M. Ko, *Nucl. Phys. A* **618**, 498 (1997).
- [79] V. Baran, A. Larionov, M. Colonna and M. Di Toro, *Nucl. Phys. A* **632**, 287 (1998).
- [80] L. Shi and P. Danielewicz, *Euro. Phys. Lett.* **49**, 34 (2000).
- [81] H.S. Xu et al., *Phys. Rev. Lett.* **85**, 716 (2000).
- [82] M. Ferreira, R. Câmara Pereira, and C. Providência, *Phys. Rev. D* **101**, 123030 (2020).
- [83] W. J. Xie and B. A. Li, *Phys. Rev. C* **103**, 035802 (2021).
- [84] S. P. Tang, J. L. Jiang, W. H. Gao, Y. Z. Fan, and D. M. Wei, *Phys. Rev. D* **103**, 063026 (2021).
- [85] Z. Miao, A. Li, Z. Zhu, and S. Han, *Astrophys. J.* **904**, 103 (2020).
- [86] R. Somasundaram and J. Margueron, *Europhysics Letters* **138**, 14002 (2022).